

# Energy Advances

Accepted Manuscript

This article can be cited before page numbers have been issued, to do this please use: Y. Yao, E. Minami and H. Kawamoto, *Energy Adv.*, 2024, DOI: 10.1039/D4YA00261J.



This is an Accepted Manuscript, which has been through the Royal Society of Chemistry peer review process and has been accepted for publication.

Accepted Manuscripts are published online shortly after acceptance, before technical editing, formatting and proof reading. Using this free service, authors can make their results available to the community, in citable form, before we publish the edited article. We will replace this Accepted Manuscript with the edited and formatted Advance Article as soon as it is available.

You can find more information about Accepted Manuscripts in the [Information for Authors](#).

Please note that technical editing may introduce minor changes to the text and/or graphics, which may alter content. The journal's standard [Terms & Conditions](#) and the [Ethical guidelines](#) still apply. In no event shall the Royal Society of Chemistry be held responsible for any errors or omissions in this Accepted Manuscript or any consequences arising from the use of any information it contains.

1 **Title page**

2

3 **Title:** Effect of process parameters on woody biomass fractionation in methanol/water  
4 mixture in a semi-flow reactor

5

6 **Type of article:** Original article

7

8 **Authorship:**

9 Yao Yilin, <sup>a</sup> Eiji Minami, <sup>\*a</sup> Haruo Kawamoto <sup>a</sup>

10 <sup>a</sup> Department of Socio-Environmental Energy Science, Graduate School of Energy Science,  
11 Kyoto University, Yoshida-honmachi, Sakyo-ku, Kyoto 606-8501, Japan

12

13 **\*Corresponding author:**

14 Eiji Minami

15 minami@energy.kyoto-u.ac.jp

16 Tel: +81-(0) 75-753-5713, Fax: +81-(0) 75-753-4736

17

18

19

20

21



## 22 Abstract

23

24 The degradation of woody biomass in methanol/water mixtures at elevated temperatures  
25 and pressures is a promising candidate for chemical production from renewable resources,  
26 combining the wood-degrading ability of water with the product-dissolving capacity of  
27 methanol. However, the effects of water and methanol on wood degradation remain unclear.  
28 In the present study, the effect of process parameters on the degradation of Japanese cedar in  
29 methanol/water at 270°C and 10–30 MPa was investigated using a semi-flow reactor in  
30 which pressure and temperature can be controlled independently. At 270°C, hemicelluloses  
31 were degraded and solubilized more preferentially at 10 MPa, but delignification was more  
32 preferred at 20 and 30 MPa. In the resulting products, methylation of coniferyl alcohol from  
33 lignin and methyl esterification of methyl glucuronopentosan from hemicellulose were more  
34 advanced at 20 and 30 MPa than at 10 MPa. These results suggest that at 10 MPa the  
35 influence of water is dominant and promotes polysaccharide degradation, whereas at 20 and  
36 30 MPa the influence of methanol is dominant and promotes delignification. Our findings  
37 will provide insight into the establishment of efficient chemical production from woody  
38 biomass with solvolysis technology.

39

40 **Keywords:** supercritical methanol; hot-compressed water; woody biomass; lignin;  
41 hemicellulose; semi-flow reactor

42



## 43 Introduction

44

45 The efficient conversion of woody biomass into valuable chemicals has always been a  
46 popular topic of research, but the strong and complex structure of wood cell walls, which  
47 comprise cellulose, hemicelluloses, and lignin, renders it difficult. Supercritical fluid  
48 technology is a candidate for wood conversion owing to its unique properties.<sup>1</sup> Owing to its  
49 high ionic product and solubility, supercritical water (critical point (CP), 374 °C and 22.1  
50 MPa) can serve as a catalyst and solvent for wood decomposition and subsequent  
51 solubilization of the resulting products, respectively.<sup>2,3</sup> However, undesirable recondensation  
52 and overdegradation of the products have been reported owing to the severe reaction  
53 conditions.<sup>4-9</sup> Therefore, wood decomposition in hot-compressed water at lower  
54 temperatures than supercritical water has been studied. Takada and Saka reported that lignin  
55 and hemicelluloses were decomposed at 230 °C and cellulose at 270 °C, but the solubility of  
56 lignin derivatives in hot-compressed water was not high, resulting in less delignification.<sup>8</sup>

57 However, methanol, which has a lower CP (239 °C and 8.1 MPa) than water, can provide  
58 more moderate reaction conditions and dissolve more lignin-derived products because it  
59 dissolves aromatics more readily.<sup>10-13</sup> Lignin can be depolymerized by  $\beta$ -ether cleavage, and  
60 even oligomers dissolve well in methanol, facilitating delignification.<sup>10</sup> Polysaccharides can  
61 also be decomposed by methanolysis to produce methylglycosides.<sup>14</sup> Owing to the excellent  
62 delignification capability of supercritical methanol, the production of aromatic chemicals in  
63 combination with catalytic hydrogenolysis and hydrogenation has been studied extensively  
64 in recent years.<sup>15-21</sup> However, we have reported that methanol is less reactive than water,



65 requiring 270 °C for the degradation of lignin and hemicelluloses, and 350 °C for cellulose.<sup>10</sup>

66 Given this situation, mixing methanol and water would combine the wood-decomposing  
67 ability of water with the product-solubilizing ability of methanol.<sup>22–27</sup> We have reported that  
68 the addition of water to methanol facilitates wood decomposition and solubilization better  
69 than neat methanol and neat water in a batch reactor, and that Japanese beech sapwood is  
70 almost completely decomposed and solubilized at 350 °C with an optimum water content of  
71 10 vol%.<sup>22</sup> Cheng et al. obtained 65 wt% bio-oil from white pine sawdust at 300 °C for 15  
72 min using 50 wt% aqueous methanol or ethanol.<sup>23</sup> Other studies have demonstrated the  
73 positive effect on wood liquefaction of adding water to alcohol, even in the presence of  
74 alkaline catalysts such as KOH and NaOH,<sup>27</sup> or heterogeneous solid catalysts such as Ru/H-  
75 Beta zeolite, Ni/Al<sub>2</sub>O<sub>3</sub>, and CuZnAl.<sup>24–27</sup> Despite such interesting studies, the effects of the  
76 physical properties of water and methanol, which change with temperature and pressure, on  
77 wood decomposition are not fully understood.

78 Semi-flow reactors allow rapid recovery of products, thereby preventing unwanted  
79 overdegradation. In recent years, the efficient production of aromatic monomers by  
80 solvolysis of lignin in a semi-flow reactor followed by catalytic hydrogenolysis and  
81 hydrogenation in a fixed bed catalyst column has been extensively studied.<sup>19–21</sup> In addition,  
82 semi-flow reactors are suitable for investigating the effects of the process parameters because  
83 they enable the independent control of temperature, pressure, and flow rate and provide time-  
84 resolved data.<sup>19</sup> In a previous study, we developed a semi-flow reactor and investigated the  
85 effect of pressure on the decomposition of Japanese cedar in supercritical methanol. We  
86 reported that high pressure enabled the solubilization of high-molecular-weight lignin-



87 derived oligomers and facilitated delignification.<sup>28</sup>

88 In the present study, we investigated the effects of solvent pressure and flow rate on the  
89 decomposition of Japanese cedar in methanol with adding 10 vol% water. The mechanism  
90 by which the decomposition took place is discussed herein to inform the establishment of  
91 sophisticated chemical production from woody biomass.

## 93 **Experimental**

### 95 **Materials**

96 Japanese cedar (*Cryptomeria japonica*) sapwood flour (NAKAWOOD Co., Ltd,  
97 Tokushima, Japan; sieved to a fraction between 100 and 35 mesh (ca. 0.15–0.5 mm in size))  
98 was extracted with acetone for 4 h using a Soxhlet apparatus, and dried overnight at 105 °C.  
99 Holocellulose, a delignified sample, was prepared from this extractive-free wood flour by  
100 repeating the Wise method<sup>29</sup> seven times, and was used for comparison to study the effect of  
101 lignin. Methanol (>99.8%, guaranteed reagent grade, Nacalai Tesque Inc., Kyoto, Japan) and  
102 deionized water prepared with a Milli-Q Integral 3 system (Merck Millipore, Burlington, MA,  
103 USA) were used as solvents.

### 105 **Semi-flow reactor**

106 Figure 1 shows a scheme of the semi-flow reactor, which we have described in detail  
107 previously.<sup>28</sup> Approximately 150 mg of the wood flour (or 100 mg of its holocellulose) was  
108 placed in a particulate filter (SS-4TF-2, 2- $\mu$ m nominal pore size; Swagelok Co., Solon, OH,



109 USA), which served as a sample holder. A methanol/water mixture was supplied with a  
110 plunger pump at a ratio of 90/10 v/v (methanol mole fraction is approximately 0.8), which  
111 was the optimum value established in our previous report,<sup>22</sup> at flow rates of 5, 10, or 20  
112 mL/min; the pressure of the mixture was set to 10, 20, or 30 MPa using a back-pressure valve.  
113 A coiled preheater and the sample holder were heated in an electric furnace. The reaction  
114 temperature, which was measured at the outlet of the sample holder, was controlled from  
115 room temperature to 270 °C at a rate of ca. 8 °C/min, and then maintained at 270 °C for 30  
116 min. Bazaev et al. reported the critical temperature and pressure of the methanol/water  
117 mixture (methanol mole fraction 0.8) as 260°C and 10.2 MPa, respectively.<sup>30</sup> In the above  
118 treatment, the methanol/water mixture is supercritical from 260 to 270°C, but is in the liquid  
119 phase from room temperature to 260°C. Therefore, the term supercritical is not used in this  
120 paper.

121 During the treatment, the wood-derived products solubilized in the methanol/water  
122 mixture flowed out of the sample holder and were collected in a glass bottle after cooling in  
123 a cooling tube; this fraction is referred to as the soluble fraction. After treatment, the sample  
124 holder was quenched by opening the furnace and increasing the solvent flow rate to 30  
125 mL/min. The solid residue in the holder was then collected and dried in an oven at 105 °C;  
126 this fraction is referred to as the insoluble residue. For comparison, treatment with neat  
127 methanol at 270 °C or neat water at 230 °C was conducted in the same manner. The reason  
128 we chose different temperatures for neat methanol and neat water is that the reactivity of  
129 wood in these solvents is different. Water at 230°C and methanol at 270°C are equivalent  
130 and can degrade hemicelluloses and lignin, but not cellulose, at these temperatures.<sup>9,10</sup> All



131 experiments were performed in duplicate, and the results are reported as averages, except for  
132 the experiments with holocellulose, neat methanol, and neat water, which were conducted  
133 for comparison.

134

### 135 *Analytical methods*

136 The lignin content of the insoluble residue was determined by the Klason method,<sup>31</sup> and  
137 is reported as the sum of the Klason lignin and the acid-soluble lignin. The cellulose and  
138 hemicellulose contents were estimated based on the composition of monosaccharides present  
139 in the hydrolysate from lignin determination with the assumption that the glucose/mannose  
140 ratio of glucomannan is 1/4 (mol/mol).<sup>32</sup> The hydrolysate was analyzed by high-performance  
141 anion-exchange chromatography (HPAEC).

142 We carried out the following analyses on the soluble fraction: HPAEC to determine  
143 saccharide yield; high-performance liquid chromatography (HPLC) to quantify lignin-  
144 derived monomers; gel permeation chromatography (GPC) to analyze the molecular weight  
145 distribution of lignin-derived oligomers; heteronuclear single quantum coherence  
146 spectroscopy (HSQC) for chemical structure analysis of lignin-derived oligomers; gas  
147 chromatography–mass spectrometry (GC–MS) for product identification, and matrix-  
148 assisted laser desorption ionization–time-of-flight mass spectrometry (MALDI–TOF/MS)  
149 for oligosaccharide analysis.

150 Because the soluble fraction contained methylated mono- and oligosaccharides as  
151 described below, the saccharide yield is reported as the monosaccharide yield after hydrolysis.  
152 For this purpose, the soluble fraction was dried under vacuum, hydrolyzed in an autoclave at





153 121 °C with 4 wt% aqueous sulfuric acid, and subjected to HPAEC analysis. To remove  
154 monomeric compounds prior to HSQC analysis, the soluble fraction was dried under vacuum  
155 and fractionated with ethyl acetate and water. The ethyl acetate fraction was then dried under  
156 vacuum, washed with *n*-hexane, and dissolved in deuterated dimethyl sulfoxide.<sup>33</sup> For GC–  
157 MS analysis, 1,3-diphenoxybenzene was added to the soluble fraction as an internal standard.  
158 The mixture was then dried under vacuum and silylated by adding hexamethyldisilazane (150  
159  $\mu$ L), trimethylchlorosilane (80  $\mu$ L), and pyridine (100  $\mu$ L) while stirring at 60 °C for 30 min.  
160 The conditions of each analysis were as follows.

161 HPLC: LC-20A (Shimadzu Corp., Kyoto, Japan); column, Cadenza CD-C18 (Imtakt Corp.,  
162 Kyoto, Japan); eluent, methanol/water = 20/80 to 100/0 (50 min); flow rate, 1.0 mL/min;  
163 ultraviolet (UV) detector, 280 nm; column temperature, 40 °C.

164 GPC: LC-20A; column, Shodex KF-803, KF-802.5, KF-802, and KF-801 (Resonac Holdings  
165 Corp., Tokyo, Japan) in series; flow rate, 0.6 mL/min; eluent, tetrahydrofuran; UV detector,  
166 280 nm; column temperature, 50 °C.

167 HPAEC: Prominence (Shimadzu Corp.); column, CarboPac PA-1 (250-mm analysis column  
168 connected with a 50 mm guard column; Thermo Fisher Scientific Inc.); eluent, 30 mM  
169 aqueous sodium hydroxide; flow rate, 1.0 mL/min; electrochemical detector (DECADE Elite,  
170 Antec Scientific, Zoeterwoude, The Netherlands); column temperature, 35 °C.

171 GC–MS: QP2010 Ultra (Shimadzu Corp.); column, CPSil 8CB (Agilent Technologies Inc.,  
172 30 m length, 0.25 mm diameter, 0.25  $\mu$ m thickness); injection temperature, 250 °C; split  
173 ratio, 10/1; column temperature, 100 °C (2 min), 4 °C/min to 220 °C, 220 °C (2 min),



174 15 °C/min to 300 °C, 300 °C (2 min); carrier gas, hydrogen; flow rate, 37.4 mL/min.  
175 MALDI–TOF/MS: AXIMA Performance (Shimadzu Corp.); linear mode; acceleration  
176 voltage, 20 kV; pulsed laser, 200 µJ per shot; matrix solution, 2,5-dihydroxy-benzoic acid  
177 (Sigma-Aldrich, Inc., St. Louis, MD, USA); sodium solution, sodium trifluoroacetate  
178 (Sigma-Aldrich, Inc.).  
179 HSQC: Varian AC-400 spectrometer (400 MHz, Varian Medical Systems, Inc., Palo Alto,  
180 CA, USA).

181

## 182 **Results and discussion**

183

### 184 *Degradation behavior of wood cell wall components*

185 Figure 2 shows the composition of the insoluble residue obtained from Japanese cedar  
186 as treated at 270 °C in methanol/water at various pressures and flow rates in comparison with  
187 untreated wood. At this temperature, cellulose did not degrade much, with >80% remaining  
188 in the residue under all conditions. Hemicelluloses and lignin were well degraded and  
189 solubilized, leaving 23.6%–48.6% and 4.9%–21.2% in the residue, respectively.

190 The hemicelluloses were less affected by the solvent flow rate, but were affected by  
191 pressure: the residual hemicelluloses were significantly reduced by approximately half at 10  
192 MPa compared with at 20 and 30 MPa. Figure 3 shows the results pertaining to of  
193 holocellulose, a delignified sample, in which cellulose was degraded to some extent along  
194 with the hemicelluloses. As in the case of cedar wood, these polysaccharide components were



195 more degraded and solubilized at 10 MPa, and the remaining cellulose and hemicelluloses  
196 were significantly reduced compared with those at 20 and 30 MPa, with little flow rate  
197 dependence.

198 Lignin was affected by both solvent pressure and flow rate (Figure 2); higher pressures  
199 and faster flow rates tended to reduce the residual lignin. We reported greater delignification  
200 at higher pressures in the case of supercritical methanol without water in a previous study,  
201 which revealed that high pressures improved the solubility of high-molecular-weight lignin-  
202 derived oligomers, thereby facilitating delignification.<sup>28</sup> This phenomenon was also expected  
203 in the water-added case and will be discussed later.

204 Figure 4 shows the results for neat methanol at 270 °C and neat water at 230 °C; under  
205 those conditions, cellulose did not degrade much. In neat methanol, more hemicelluloses  
206 (approximately 60%) and lignin (28.3%–51.1%) remained in the residue compared with in  
207 the water-added methanol case. Therefore, it is obvious that the addition of 10 vol% water  
208 facilitated their degradation and solubilization. Although delignification is facilitated at high  
209 pressures in neat methanol, the degradation of hemicelluloses is not pressure dependent.  
210 Therefore, in the methanol/water mixture, the pressure dependence of delignification can be  
211 attributed to methanol, whereas that of hemicellulose degradation might be due to water. In  
212 neat water (Figure 4b), the hemicelluloses were almost completely degraded and solubilized,  
213 leaving little residue, whereas more lignin remained in the residue than in neat methanol and  
214 methanol/water mixture. This comparison of the results for water and methanol shows that  
215 methanol is favorable for delignification, and water is preferred for polysaccharide  
216 degradation.



217 Figure 5 shows GPC chromatograms of the soluble fractions obtained from the treatment  
218 of cedar wood in the methanol/water mixture, compared with the neat methanol and neat  
219 water cases. Note that the chromatograms were recorded with a UV detector to provide a  
220 rough estimate of the molecular weight distribution of the lignin-derived products that  
221 absorbed UV light. The concentration of the soluble fraction decreased in inverse proportion  
222 to the flow rate, i.e., the solvent volume decreased the detection intensity during GPC  
223 analysis. Therefore, for direct comparison, the vertical axis of the chromatograms was given  
224 as the product of the detection intensity and the solvent volume but is hereafter simply  
225 referred to as intensity.

226 The chromatograms show that the molecular weight was distributed from the monomeric  
227 region (ca. 180 or less) to over 2960 in polystyrene equivalents. At a constant flow rate of 5  
228 mL/min (Figure 5a), the intensity in the high molecular weight region (from ca. 1270 to above  
229 2960) increased with increasing pressure. This indicates that the facilitated delignification at  
230 high pressures (Figure 2) was due to the dissolution of high-molecular-weight lignin-derived  
231 products, as already suggested in the case of neat methanol (Figure 5c).<sup>28</sup> In the case of neat  
232 water (Figure 5d), the molecular weight distribution did not change with increasing pressure.  
233 Therefore, it is clear that the facilitated delignification at high pressures originates from  
234 methanol, not water.

235 At a constant pressure of 10 MPa (Figure 5b), the shape of the molecular weight  
236 distribution did not change much, but the intensity tended to increase in the entire molecular  
237 weight region with increasing flow rate. This increased intensity can be attributed to the  
238 increase in solvent volume proportional to the flow rate, which dissolved more lignin-derived



239 products. This may be the reason for the improved delignification with increasing flow rate  
240 (Figure 2). However, the hemicelluloses were not affected by the solvent flow rate in Figure  
241 2, probably because the slow decomposition of polysaccharides in methanol was the limiting  
242 factor rather than solubility.

243 As described above, the changes in the molecular weight distribution in Figure 5 with  
244 the solvent pressure and flow rate correspond well to the degradation behavior of lignin in  
245 Figure 2. In the methanol/water mixture, because delignification was enhanced at 20 and 30  
246 MPa, and polysaccharide degradation was promoted at 10 MPa, the properties of methanol  
247 seemed to dominate at 20 and 30 MPa, and those of water at 10 MPa.

248

### 249 *Characterization of lignin-derived products*

250 Figure 6 shows the HSQC spectra of lignin-derived oligomers in the soluble fraction  
251 obtained from Japanese cedar as treated in methanol/water at 10 and 30 MPa, with the  
252 corresponding chemical structures. Because  $\beta$ -O-4 (A), pinoresinol (B), and phenylcoumaran  
253 (C) structures were found, the lignin-derived oligomers retained the original lignin structures  
254 to some extent. In addition, methylation of the  $\alpha$ -hydroxy group of the  $\beta$ -O-4 structure (A')  
255 and the  $\gamma$ -hydroxy group of the coniferyl alcohol unit (F) was observed under the influence  
256 of methanol.

257 The spectra do not reveal any significant difference between the 10 and 30 MPa cases,  
258 indicating that pressure had little effect on the chemical structures of the lignin-derived  
259 oligomers, and that the facilitated delignification at 30 MPa was only owing to the improved  
260 solubility, as suggested by the GPC analysis reported in Figure 5. Furthermore, the HSQC



261 spectra do not differ significantly from the case of neat methanol,<sup>28</sup> indicating that the  
262 addition of 10 vol% water affected the degree of delignification, but not the chemical  
263 structures of the lignin-derived products. Note that Andersen et al. also reported similar  
264 HSQC spectra when poplar was treated with neat methanol at 190°C and 6 MPa, although in  
265 this case hydrogen gas was introduced simultaneously.<sup>19</sup>

266 Figure 7 shows the GC–MS chromatograms of the soluble fractions. The major peaks of  
267 the lignin-derived monomers were attributable to coniferyl alcohol (CA, **15**) and its  $\gamma$ -methyl  
268 ether (CA- $\gamma$ , **6**). CA is the primary product of the radical cleavage of  $\beta$ -ether bonds via  
269 quinone methide intermediates.<sup>20,34–36</sup> It is also formed by the supercritical methanol  
270 treatment of dimeric  $\beta$ -O-4 lignin model compounds.<sup>37</sup> Free CA can be converted to CA- $\gamma$  in  
271 supercritical methanol,<sup>37</sup> and can also be formed prior to  $\beta$ -ether cleavage, as confirmed by  
272 HSQC in the present study (Figure 6). Similar  $\gamma$ -esterified CAs have been reported to be  
273 formed in other monohydric (e.g., ethanol and 1-propanol) or dihydric (1,3-butanediol)  
274 alcohols.<sup>11,35</sup> Vanillin (**1**), isoeugenol (IE, **2**), dihydroconiferyl alcohol (DHCA, **8**), and  
275 coniferyl aldehyde (CAld, **9**) were also detected in small quantities.

276 The quantification results shown in Table 1 indicate that CA and CA- $\gamma$  accounted for at  
277 least >60% of the lignin-derived monomers identified in the methanol/water treatment. The  
278 total monomer yield was higher at lower pressures and slower flow rates. For example, at 10  
279 MPa and 5 mL/min, the total monomer yield peaked at 19.1 wt% based on lignin, but reached  
280 a minimum of 11.4 wt% at 30 MPa and 20 mL/min. This trend was the opposite to that of  
281 delignification, which was more favorable at higher pressures and faster flow rates, as shown  
282 in Figure 2. The HSQC spectra (Figure 6) show that the  $\beta$ -O-4 structures still remained in the



283 lignin-derived oligomers in the soluble fraction. These  $\beta$ -ether bonds can be further cleaved  
284 to form more monomers if the oligomers take longer to reach the cooling tube. Higher  
285 pressures would extract oligomers from the wood cell walls more efficiently, and faster flow  
286 rates would allow oligomers to flow more quickly from the reactor into the cooling tube,  
287 thereby suppressing cleavage of these remaining  $\beta$ -ether bonds and decreasing the formation  
288 of monomers. This may be the reason for the opposite trends in monomer yield and  
289 delignification.

290 The conversion of CA to CA- $\gamma$  tended to be pronounced at higher pressures and slower  
291 flow rates. For example, at 10 MPa and 20 mL/min, the CA- $\gamma$ /CA ratio had a minimum value  
292 of  $1.2/11.4 = 0.11$ , whereas at 30 MPa and 5 mL/min, it peaked at  $3.4/7.9 = 0.43$ . The  
293 conversion to CA- $\gamma$  may increase owing to the long residence time in the reactor at slow flow  
294 rates, and also increase owing to the marked influence of methanol at high pressures. In Table  
295 1, the CA- $\gamma$ /CA ratio is higher for neat methanol compared with the water-added methanol  
296 cases, whereas CA- $\gamma$  was not produced in neat water, as expected.

297 CAld, IE, and DHCA are possible pyrolysis products of CA, and quinone methide and  
298 radical mechanisms have been proposed as pathways for their formation.<sup>38</sup> CAld formation  
299 occurred less in neat methanol and more in neat water, and CAld formation in water-added  
300 methanol was similar to, or slightly less than, that in neat water. Conversely, the IE yield was  
301 higher in neat methanol, lower in water-added methanol, and undetectable in neat water.  
302 DHCA was detected to some extent in neat methanol and neat water, but less so in water-  
303 added methanol. It is difficult to produce vanillin from CA. Therefore, it is probably produced  
304 by some other mechanism. For example, vanillin is one of the acidolysis products of lignin,



305 and is also found in small amounts in subcritical water or steam explosion treatment.<sup>9,39</sup>  
306 Although it is interesting that the selectivity of the formation of these minor products changes  
307 with the type of solvent, there are insufficient experimental data for a full discussion of this  
308 in the present study.

309

### 310 *Characterization of polysaccharide-derived products*

311 Cellulose was relatively stable at 270 °C in methanol/water (Figure 2). Therefore, we  
312 expected most of the polysaccharide-derived products to have originated from hemicelluloses.  
313 The main monosaccharides detected in the GC–MS spectra (Figure 7) were methyl  
314 glycosides, such as methyl-D-xylopyranosides (**3** and **4**), methyl-D-mannopyranosides (**7** and  
315 **10**), methyl-D-galactopyranosides (**11** and **12**), and methyl-D-glucopyranosides (**13** and **14**),  
316 but they were present in low levels, and sugar-derived products such as furfural and 5-  
317 hydroxymethylfurfural were not detected. Therefore, most of the polysaccharide-derived  
318 products were probably oligosaccharides.

319 Figure 8 shows the MALDI–TOF/MS spectra of the soluble fractions from Japanese  
320 cedar holocellulose treated in the methanol/water mixture. We have included the  
321 holocellulose data because the soluble fraction from the Japanese cedar wood was difficult  
322 to analyze by MALDI–TOF/MS, probably due to the presence of lignin. The products were  
323 detected as sodium-added ions (+23) because a sodium solution was used with the matrix.  
324 Based on the mass-to-charge ratios, we detected peaks attributable to the 132 m/z (pentose  
325 unit) intervals of +32 (OCH<sub>3</sub>+H) and +23 (Na-added) (e.g., 1111.5 and 1243.5), which can  
326 be assigned to pentosans with a methylated reducing end (P<sub>n</sub>Me). Peaks attributable to methyl





327 glucuronic acid (+190, P<sub>n</sub>Me(MG), e.g., 1037.5 and 1169.5) or its methyl ester (+204,  
328 P<sub>n</sub>Me(MGMe), e.g., 1051.5 and 1183.5) added to the pentosan were also observed. These  
329 peaks can be assigned to oligosaccharides produced from arabino-4-*O*-  
330 methylglucuronoxylan by methanolysis, of which some methyl glucuronic acid residues were  
331 methyl esterified under the influence of methanol. It is interesting to note that the peaks  
332 attributable to pentosans with methyl-esterified methyl glucuronic acid (P<sub>n</sub>Me(MGMe))  
333 increased with increasing pressure. This result also supports the intense effect of methanol at  
334 high pressures. Although methylated hexosans from acetylgalactoglucomanan or cellulose  
335 were not detected by MALDI-TOF/MS, they are considered to be present in the soluble  
336 fractions as well as the pentosans, according to the sugar analysis below.

337 The formation of oligosaccharides with few monosaccharides may be due to a feature of  
338 the semi-flow reactor that enables the rapid flow of the products from the reactor and their  
339 recovery as oligosaccharides before decomposition to monomers. Similarly, the formation of  
340 oligosaccharides with reducing ends by hydrolysis has also been reported in hot-compressed  
341 water treatment with a semi-flow reactor. However, in the present study, no oligosaccharides  
342 with reducing ends were detected, despite the presence of water. This may have been because  
343 hydrolysis did not proceed well with only 10% water, and/or the unstable reducing ends were  
344 rapidly methylated or degraded. We expected hydrolysis to be involved in the mechanism,  
345 but only methylglycosides derived from methanolysis were detected, with almost no  
346 hydrolysis products. Therefore, the mechanism by which the addition of water promotes  
347 wood degradation remains unclear.

348 To quantify the recovered saccharides, the soluble fractions from Japanese cedar wood



349 were hydrolyzed, and the yields of the resulting monosaccharides are shown in Table 2.  
350 Glucose (Glu), mannose (Man), galactose (Gala), xylose (Xyl), and arabinose (Ara) were  
351 present as constituent sugars. Therefore, it is clear that galactoglucomannan-derived  
352 hexosans were present in the soluble fraction, as well as arabinoxylan-derived pentosans.

353 Table 2 also shows the percentages of solubilized products from polysaccharide  
354 components in the Japanese cedar, as estimated from the results in Figure 2. Cellulose was  
355 degraded less in methanol/water at 270 °C, but the hemicelluloses were degraded and  
356 solubilized most at 10 MPa, resulting in the highest percentage of solubilized products: 33.4  
357 wt% based on the original polysaccharide mass in the cedar wood. However, the total  
358 monosaccharide yield was only 9.7 wt%, which was lower than at 30 MPa. This indicates  
359 that most of the solubilized saccharides were further decomposed to other products at 10 MPa  
360 compared with at 30 MPa. Similarly, in the case of neat methanol, the total monosaccharide  
361 yield decreased with decreasing pressure. As explained below, the densities of neat methanol  
362 and the methanol/water mixture decrease significantly at 10 MPa at 270 °C (ca. 130 kg/m<sup>3</sup>,  
363 respectively),<sup>30,40</sup> resulting in poor solubility, which could prevent rapid solubilization of  
364 oligosaccharides from wood cell walls and lead to overdecomposition. In the case of neat  
365 water, the density did not change much with pressure (774 kg/m<sup>3</sup> at 10 MPa and 798 kg/m<sup>3</sup>  
366 at 30 MPa) at 270 °C,<sup>41</sup> and the total monosaccharide yield was high, even at 10 MPa.

367

### 368 *Effects of solvent density on wood degradation*

369 As described in the experimental section, the Japanese cedar wood was treated in  
370 methanol/water by raising the temperature to 270 °C at ca. 8 °C/min, and the temperature



371 was maintained at 270 °C for 30 min. During the treatment, the soluble fraction was collected  
372 every 3 min and subjected to GPC analysis to determine changes in the molecular weight  
373 distribution of the lignin-derived products over the treatment time. The results are shown in  
374 Figure 9. The figure shows the changes in temperature (a) and the corresponding changes in  
375 (b) the density of the methanol/water (90/10, v/v) mixture, (c) the total intensity, and (d) the  
376 average molecular weight, as determined by GPC analysis.

377 The density of the methanol/water mixture was calculated using the Bazaev equation,<sup>30</sup>  
378 but at temperatures below 250°C, where this equation is not applicable, the density was  
379 instead calculated using the Soave-Redlich-Kwong model with a steady-state process  
380 simulator (ProII 2023, AVEVA Group plc., Cambridge, UK). The total intensity ( $I_T$ ) was  
381 obtained by integrating the intensity ( $I$ ) of the UV detector over the analysis time (0–70 min)  
382 in a GPC chromatogram, and served as an index of the amount of solubilized lignin-derived  
383 products. The average molecular weight ( $M_{av}$ ) was defined as the average value of the  
384 molecular weight ( $M$ ) weighted by the detection intensity ( $I$ ) as follows:

$$385 \quad M_{av} = \int_{0min}^{70min} (M \times I) dt / I_T \quad (1)$$

386 The relationship between the molecular weight of the polystyrene ( $M$ ) and its elution time ( $t$ )  
387 obtained from the GPC analysis fitted the following equation with an R-squared value of 0.99,  
388 which was applied to equation (1).

$$389 \quad \log_{10}M = -0.0865t + 7.4272 \quad (2)$$

390 In Figure 9, while the temperature changed from 150 °C to approximately 250 °C, the  
391 methanol/water density changed little, with no significant difference between 10 and 30 MPa  
392 (approximately 500–700 kg/m<sup>3</sup>). The total intensity began to increase at approximately



393 200 °C, indicating that the lignin had begun to degrade and leach out of the cell walls. At this  
394 time, there was no difference in total intensity between 10 and 30 MPa, but when the  
395 temperature reached approximately 270 °C, the total intensity at 30 MPa became higher than  
396 that at 10 MPa. Similarly, there was no difference in the average molecular weight between  
397 10 and 30 MPa before reaching 270 °C, but the difference became apparent at approximately  
398 270 °C.

399 These behaviors can be attributed to the fact that the high-molecular-weight lignin-  
400 derived oligomers were solubilized more at 30 MPa than at 10 MPa, as shown in Figure 5,  
401 and this seems to correspond well with the change in methanol/water density in Figure 9. The  
402 density of the methanol/water mixture at 270 °C and 10 MPa decreased to 127 kg/m<sup>3</sup>, which  
403 could be considered gas-like, limiting the solubilization of high-molecular-weight lignin-  
404 derived oligomers. In contrast, at 30 MPa, the density of methanol/water was kept at 548  
405 kg/m<sup>3</sup>, which could be considered liquid-like, thus preserving the solubility capacity.

406 Similarly, during the treatment of Japanese cedar wood, the soluble fraction was  
407 collected every minute, and the resulting changes in yields of lignin-derived monomers are  
408 shown in Figure 10. The formation of CA appeared at approximately 200 °C, and the yield  
409 of CA at 10 MPa became higher than that at 30 MPa from approximately 250 °C. At the same  
410 time, the yield of CA- $\gamma$  at 30 MPa became higher than that at 10 MPa from approximately  
411 250 °C. The large decrease in the density of methanol/water mostly started at 250 °C at 10  
412 MPa as shown in Figure 9. In this situation, we think the influence of methanol was weakened,  
413 resulting in suppressed methylation of CA. In addition, the low solvent density shortened its  
414 residence time, which also suppressed the conversion of CA to CA- $\gamma$ . However, the total



415 yield of CA and CA- $\gamma$  was not significantly different between 10 and 30 MPa, indicating that  
416 pressure did not significantly affect the formation of CA, a primary product of  $\beta$ -ether  
417 cleavage, but only the conversion of CA to CA- $\gamma$ .

418

## 419 **Conclusions**

420

421 In the present study, Japanese cedar wood was treated with the methanol/water mixture  
422 (90/10, v/v) at 270 °C and 10, 20, or 30 MPa using a semi-flow reactor to reveal the effect of  
423 process parameters on its degradation. The main findings were as follows.

- 424 ● Cellulose was not degraded significantly at 270 °C, but the degradation and  
425 solubilization of hemicelluloses proceeded preferentially at 10 MPa, but delignification  
426 was more preferred at 20 and 30 MPa.
- 427 ● At 20 and 30 MPa, high-molecular-weight lignin-derived oligomers were dissolved more  
428 in the soluble fraction than at 10 MPa, resulting in facilitated delignification.
- 429 ● In the resulting products, the conversion of coniferyl alcohol to its  $\gamma$ -methyl ether and  
430 the methyl esterification of methyl glucuronopentosan were more progressed at 20 and  
431 30 MPa than at 10 MPa.

432 In neat methanol, efficient degradation and solubilization of lignin occurred along with  
433 methyl esterification of the resulting products. Conversely, hemicellulose degradation was  
434 more prevalent in neat water. A comparison of these results suggests that in the  
435 methanol/water mixture, the influence of methanol is more pronounced at 20 MPa and 30  
436 MPa, while that of water dominates at 10 MPa. These results demonstrate that the behavior



437 of the methanol/water mixture can be modulated by adjusting the process parameters.  
438 However, the specific mechanisms underlying these effects were not elucidated within the  
439 scope of this study.

440

### 441 **Author Contributions**

442 YY and EM designed the study and evaluated the experimental data; YY performed the  
443 experiments and chemical analysis of the products, and drafted the manuscript; EM and HK  
444 supervised the study, and reviewed and edited the manuscript. All authors have read and  
445 approved the final version of the manuscript.

446

### 447 **Conflicts of interest**

448 There are no conflicts to declare.

449

### 450 **Acknowledgments**

451 We appreciate grants from the JST Mirai Program (JPMJMI20E3), JSPS KAKENHI  
452 (22K05765), and the Iwatani Naoji Foundation. We thank Edanz (<https://jp.edanz.com/ac>)  
453 for editing a draft of this manuscript.

454



455 **Footnotes**

456 <sup>a</sup> Department of Socio-Environmental Energy Science, Graduate School of Energy Science,  
457 Kyoto University, 606-8501, Yoshida-honmachi, Sakyo-ku, Kyoto, Japan. Email:  
458 minami@energy.kyoto-u.ac.jp

460 **References**

- 461 1 C. A. Eckert, B. L. Knutson and P. G. Debenedetti, *Nature*, 1996, **383**, 313–318.
- 462 2 D. Bröll, C. Kaul, A. Krämer, P. Krammer, T. Richter, M. Jung, H. Vogel and P.  
463 Zehner, *Angew. Chemie - Int. Ed.*, 1999, **38**, 2998–3014.
- 464 3 A. Kruse and E. Dinjus, *J. Supercrit. Fluids*, 2007, **41**, 361–379.
- 465 4 T. Adschiri, S. Hirose, R. Malaluan and K. Arai, *J. Chem. Eng. Japan*, 1993, **26**, 676–  
466 680.
- 467 5 N. Akiya and P. E. Savage, *Chem. Rev.*, 2002, **102**, 2725–2750.
- 468 6 K. Ehara and S. Saka, *Cellulose*, 2002, **9**, 301–311.
- 469 7 Y. Yu, X. Lou and H. Wu, *Energy and Fuels*, 2008, **22**, 46–60.
- 470 8 M. Takada and S. Saka, *J. Wood Sci.*, 2015, **61**, 299–307.
- 471 9 N. Phaiboonsilpa, K. Yamauchi, X. Lu and S. Saka, *J. Wood Sci.*, 2010, **56**, 331–338.
- 472 10 E. Minami and S. Saka, *J. Wood Sci.*, 2003, **49**, 73–78.
- 473 11 J. Yamazaki, E. Minami and S. Saka, *J. Wood Sci.*, 2006, **52**, 527–532.
- 474 12 S. Gillet, M. Aguedo, L. Petitjean, A. R. C. Morais, A. M. Da Costa Lopes, R. M.  
475 Łukasik and P. T. Anastas, *Green Chem.*, 2017, **19**, 4200–4233.



- 476 13 L. Shuai and J. Luterbacher, *ChemSusChem*, 2016, **9**, 133–155.
- 477 14 Y. Ishikawa and S. Saka, *Cellulose*, 2001, **8**, 189–195.
- 478 15 K. Barta, T. D. Matson, M. L. Fettig, S. L. Scott, A. V. Iretskii and P. C. Ford, *Green*  
479 *Chem.*, 2010, **12**, 1640–1647.
- 480 16 K. Barta and P. C. Ford, *Acc. Chem. Res.*, 2014, **47**, 1503–1512.
- 481 17 P. H. Galebach, D. J. McClelland, N. M. Eagan, A. M. Wittrig, J. S. Buchanan, J. A.  
482 Dumesic and G. W. Huber, *ACS Sustain. Chem. Eng.*, 2018, **6**, 4330–4344.
- 483 18 D. J. McClelland, P. H. Galebach, A. H. Motagamwala, A. M. Wittrig, S. D. Karlen,  
484 J. S. Buchanan, J. A. Dumesic and G. W. Huber, *Green Chem.*, 2019, **21**, 2988–3005.
- 485 19 E. M. Anderson, M. L. Stone, R. Katahira, M. Reed, G. T. Beckham and Y. Román-  
486 Leshkov, *Joule*, 2017, **1**, 613–622.
- 487 20 I. Kumaniaev, E. Subbotina, J. Sävmarker, M. Larhed, M. Galkin and J. S. Samec,  
488 *Green Chem.*, 2017, **19**, 5767–5771.
- 489 21 J. H. Jang, D. G. Brandner, R. J. Dreiling, A. J. Ringsby, J. R. Bussard, L. M. Stanley,  
490 R. M. Happs, A. S. Kovvali, J. I. Cutler, T. Renders, J. R. Bielenberg, Y. R. Leshkov  
491 and G. T. Beckham, *Joule*, 2022, **6**, 1859–1875.
- 492 22 E. Minami and S. Saka, *J. Wood Sci.*, 2005, **51**, 395–400.
- 493 23 S. Cheng, I. DCruz, M. Wang, M. Leitch and C. Xu, *Energy and Fuels*, 2010, **24**,  
494 4659–4667.
- 495 24 S. Cheng, C. Wilks, Z. Yuan, M. Leitch and C. Xu, *Polym. Degrad. Stab.*, 2012, **97**,  
496 839–848.
- 497 25 P. T. Patil, U. Armbruster and A. Martin, *J. Supercrit. Fluids*, 2014, **93**, 121–129.





- 498 26 C. Zhou, X. Zhu, F. Qian, W. Shen, H. Xu, S. Zhang and J. Chen, *Fuel Process.*  
499 *Technol.*, 2016, **154**, 1–6.
- 500 27 A. Yerrayya, A. K. Shree Vishnu, S. Shreyas, S. R. Chakravarthy and R. Vinu,  
501 *Energies*, 2020, **13**, 1–19.
- 502 28 Y. Yilin, E. Minami and H. Kawamoto, *J. Wood Sci.*, 2023, **69**, 26.
- 503 29 L. E. Wise, *Pap. trade J.*, 1946, **122**, 35–43.
- 504 30 A. R. Bazaev, B. K. Karabekova and A. A. Abdurashidova, *Russ. J. Phys. Chem. B*,  
505 2013, **7**, 955–967.
- 506 31 C. W. Dence, in *Methods in Lignin Chemistry*, Springer Verlag, Berlin, 1992, pp. 33–  
507 58.
- 508 32 X. Zhou, W. Li, R. Mabon and L. J. Broadbelt, *Energy Technol.*, 2017, **5**, 52–79.
- 509 33 J. Wang, E. Minami and H. Kawamoto, *ChemistryOpen*, 2022, **11**, e202200104.
- 510 34 S. Li, K. Lundquist and U. Westermark, *Nord. Pulp Pap. Res. J.*, 2000, **15**, 292–299.
- 511 35 T. Kishimoto and Y. Sano, *Holzforschung*, 2001, **55**, 611–616.
- 512 36 T. Kishimoto and Y. Sano, *Holzforschung*, 2002, **56**, 623–631.
- 513 37 J. Tsujino, H. Kawamoto and S. Saka, *Wood Sci. Technol.*, 2003, **37**, 299–307.
- 514 38 T. Kotake, H. Kawamoto and S. Saka, *J. Anal. Appl. Pyrolysis*, 2013, **104**, 573–584.
- 515 39 M. Tanahashi, *Bull. Wood Res. Inst. Kyoto Univ.*, 1990, **77**, 49–117.
- 516 40 R. D. Goodwin, *J. Phys. Chem. Ref. Data*, 1987, **16**, 799–892.
- 517 41 W. Wagner and A. Pruß, *J. Phys. Chem. Ref. Data*, 2002, **31**, 387–535.



## Data Availability Statement

"The data supporting this article have been included in the Supplementary Information."



## List of figures

Figure 1. Scheme of the semi-flow reactor.

Figure 2. Composition of the insoluble residue after the treatment of Japanese cedar wood with methanol/water (90/10, v/v) from room temperature to 270 °C (8 °C/min) and at 270 °C for 30 min at various flow rates and pressures (values in parentheses are percentages of the composition of untreated wood).

Figure 3. Composition of the insoluble residue after the treatment of holocellulose with methanol/water (90/10, v/v) from room temperature to 270 °C (8 °C/min) and at 270 °C for 30 min at various flow rates and pressures.

Figure 4. Composition of the insoluble residue after the treatment of Japanese cedar wood with neat methanol (from room temperature to 270 °C (8 °C/min) and at 270 °C for 30 min) or neat water (from room temperature to 230 °C (8 °C/min) and at 230 °C for 30 min) at various pressures.

Figure 5. Gel permeation chromatograms of the soluble fractions after the treatment of Japanese cedar wood under various conditions (UV detection at 280 nm).

Figure 6. Heteronuclear single quantum coherence spectra of lignin-derived oligomers



obtained from Japanese cedar wood treated with methanol/water (90/10, v/v) at 10 and 30 MPa, with the corresponding chemical structures.

Figure 7. Gas chromatography–mass spectrometry chromatograms of the soluble fractions obtained from Japanese cedar wood after treatment with methanol/water (90/10, v/v) at various pressures.

Figure 8. Matrix-assisted laser desorption ionization–time-of-flight mass spectra of oligosaccharides obtained from holocellulose after treatment with methanol/water (90/10, v/v) at various pressures.

Figure 9. Changes in (a) treatment temperature, (b) density of methanol/water (90/10, v/v), (c) total intensity, and (d) average molecular weight of lignin-derived products estimated by gel permeation chromatography (GPC) analysis during the treatment of Japanese cedar wood with methanol/water at 10 or 30 MPa at a flow rate of 5 mL/min.

Figure 10. Changes in (a) treatment temperature and (b) the yields of lignin-derived monomers during the treatment of Japanese cedar wood with methanol/water (90/10, v/v) at 10 or 30 MPa at a flow rate of 5 mL/min.



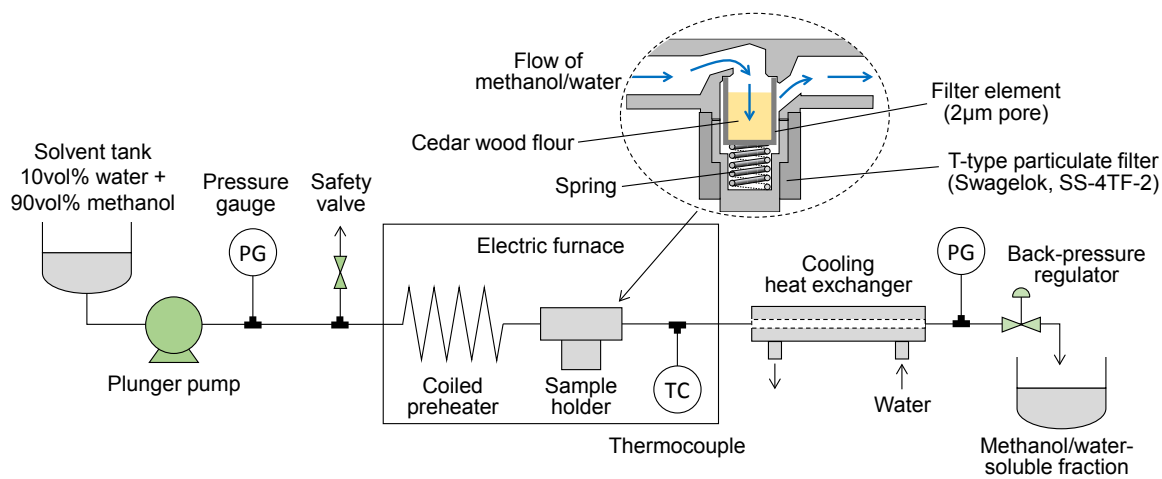


Figure 1



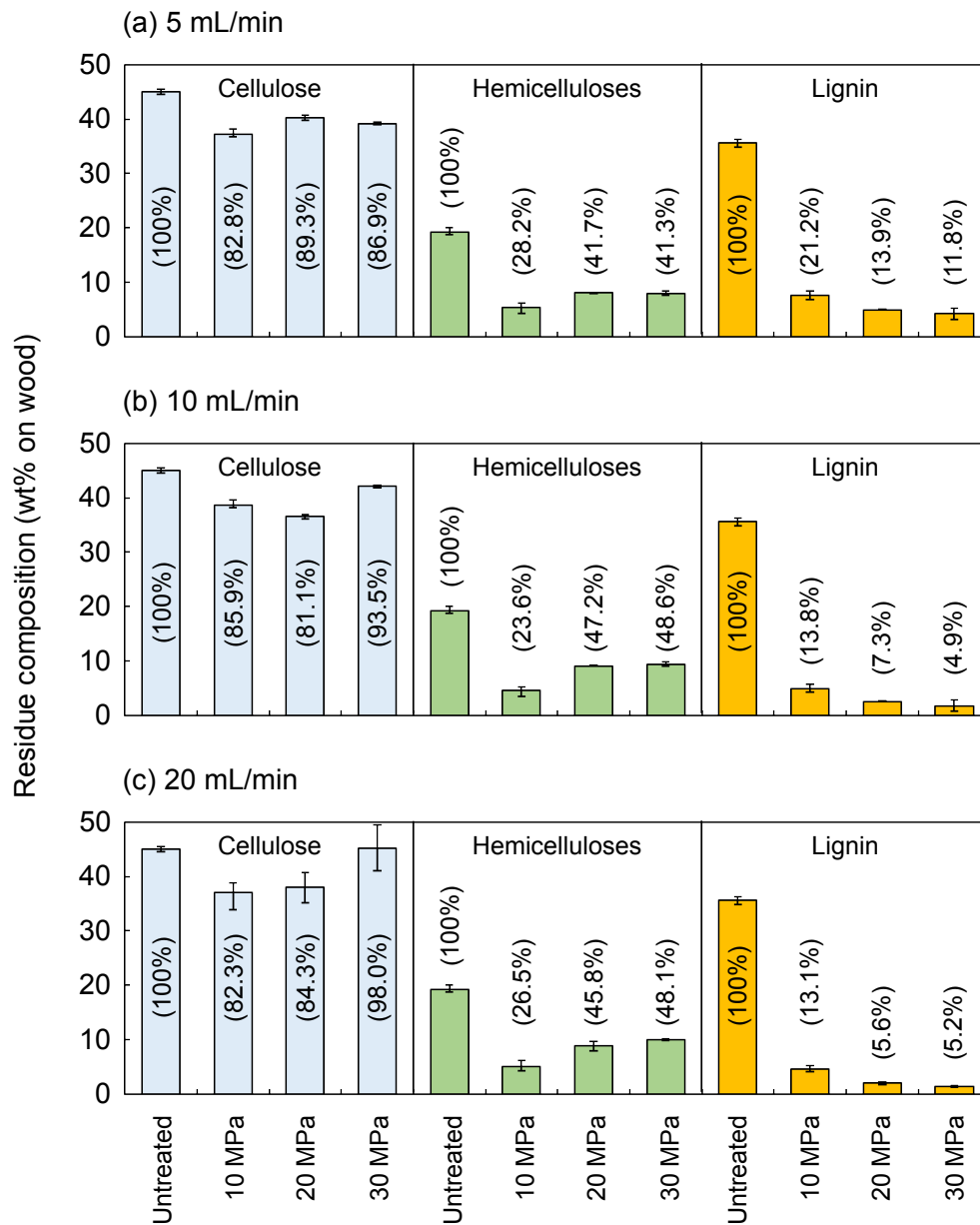


Figure 2



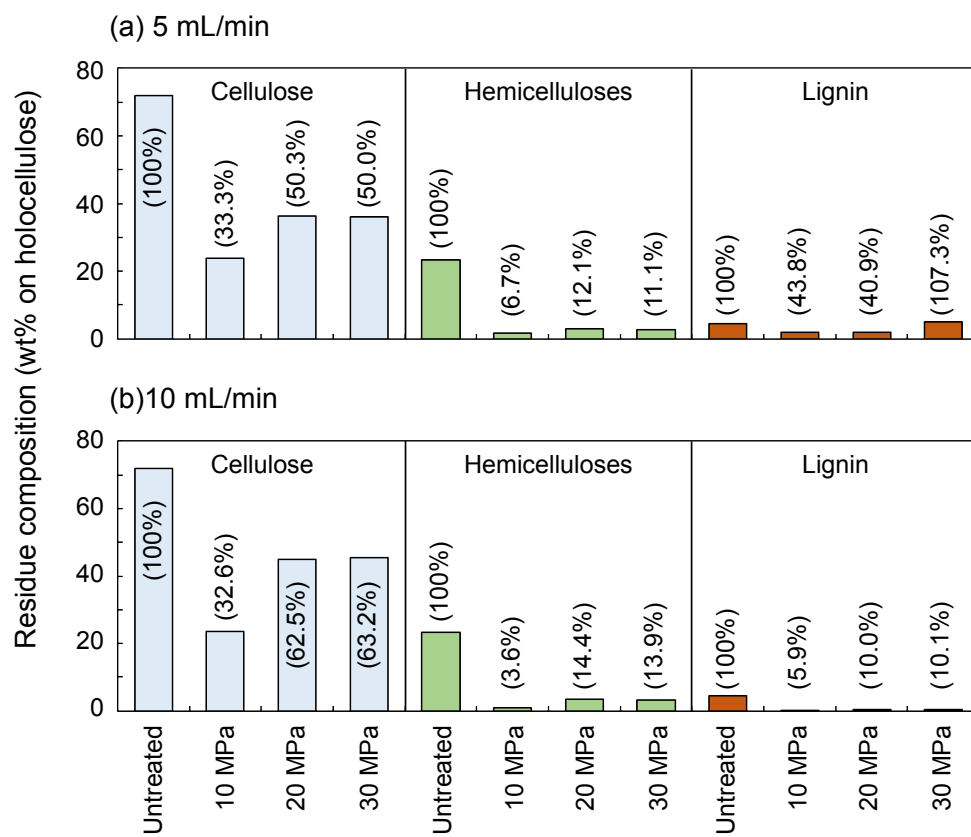


Figure 3



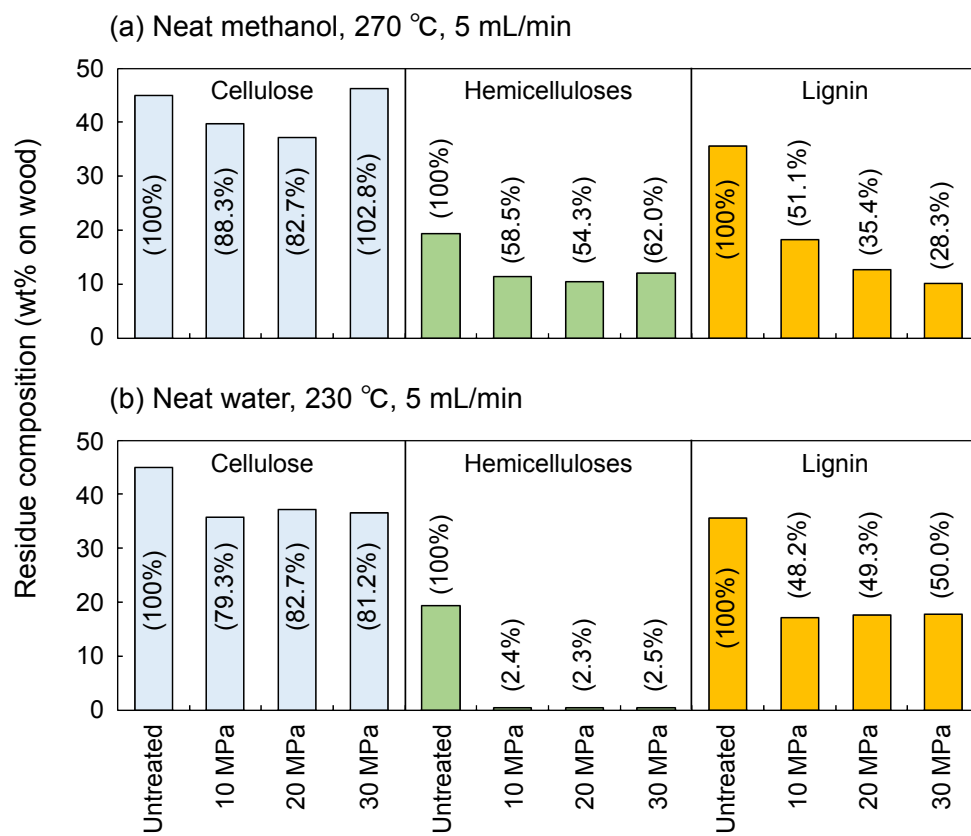


Figure 4





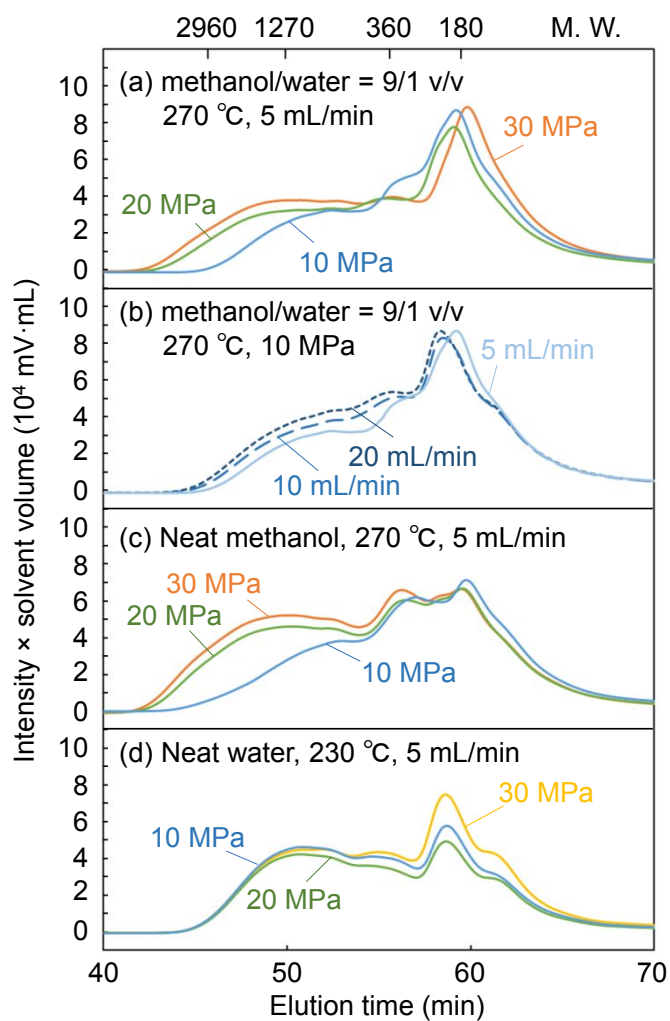


Figure 5



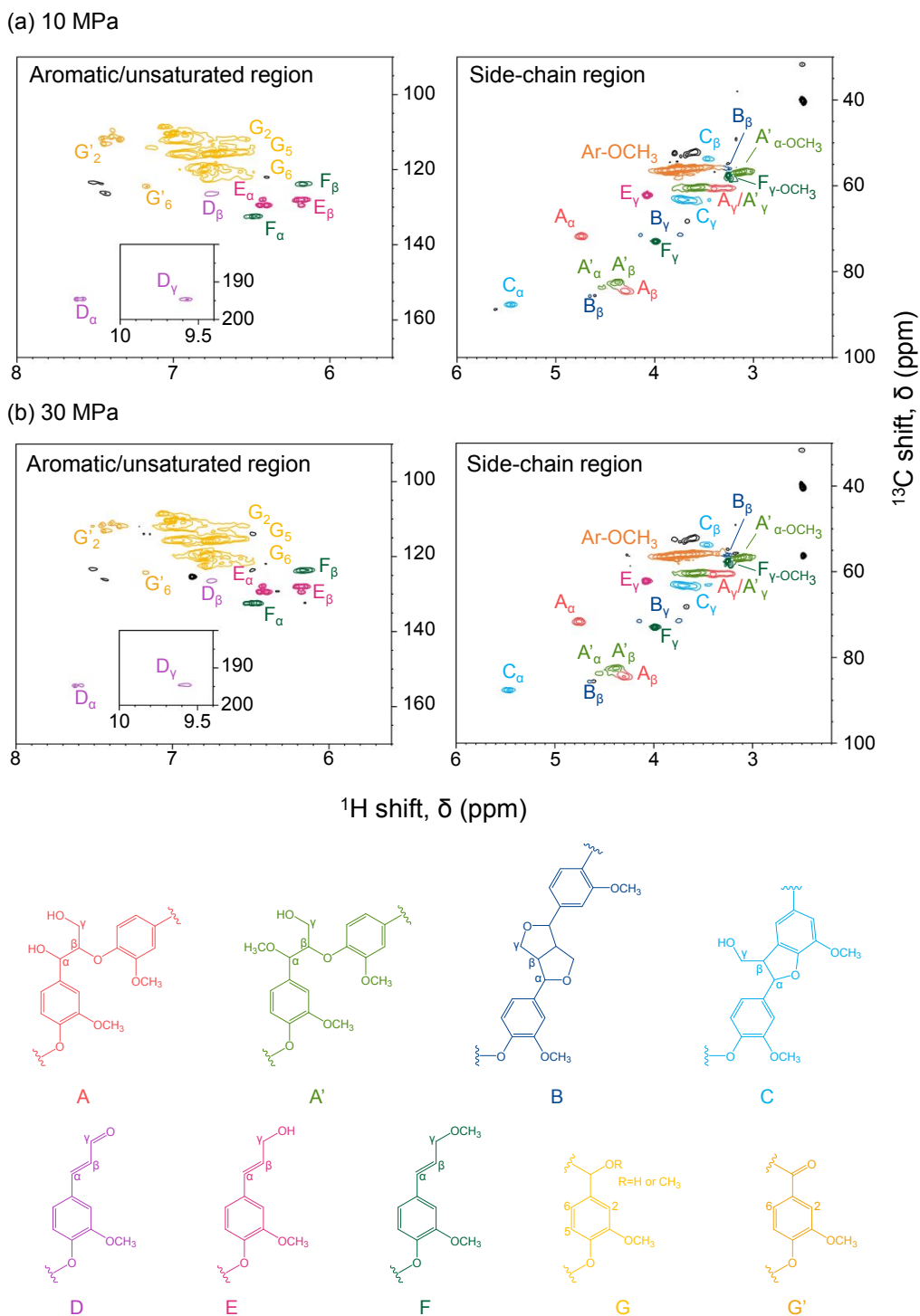


Figure 6



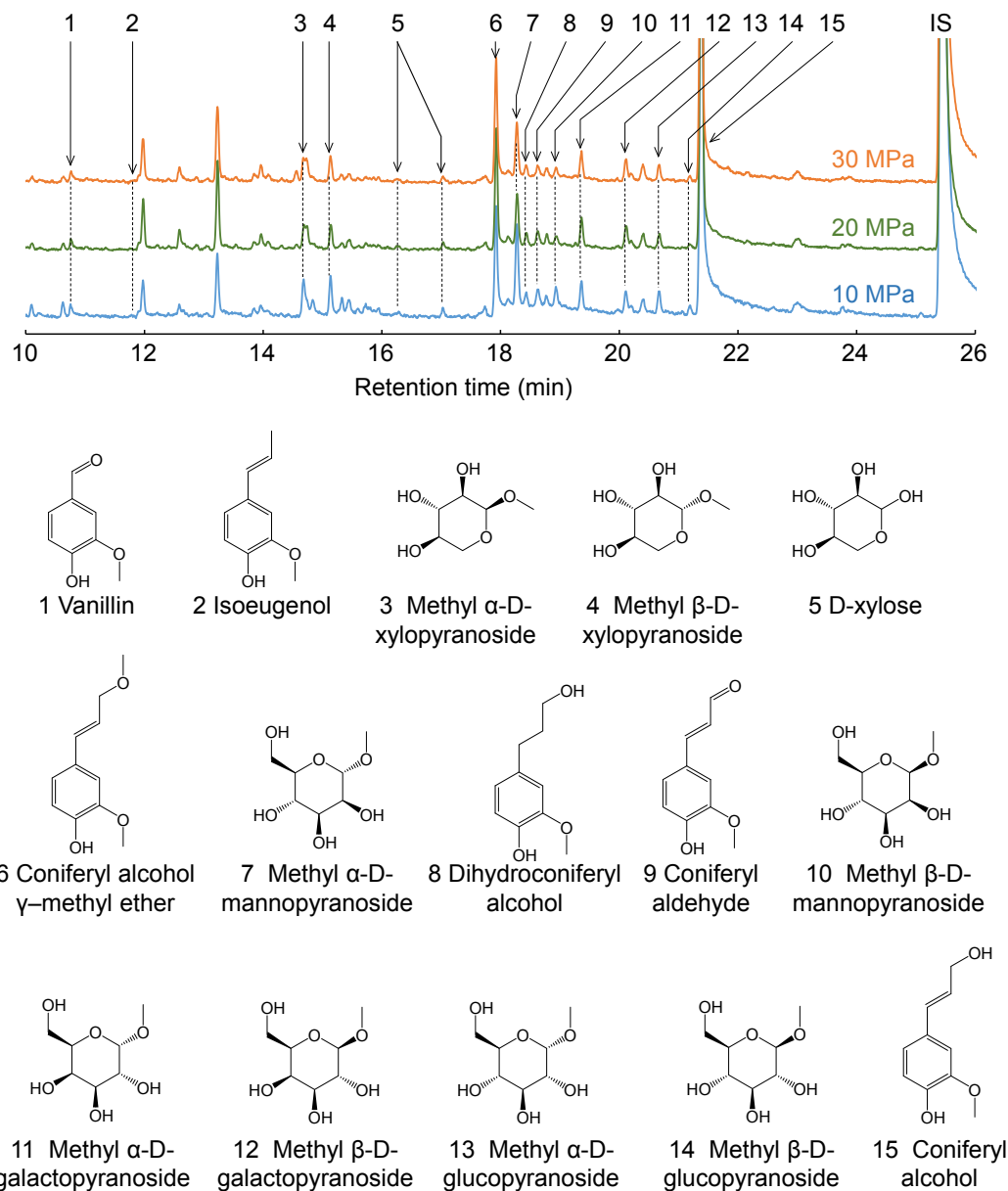


Figure 7



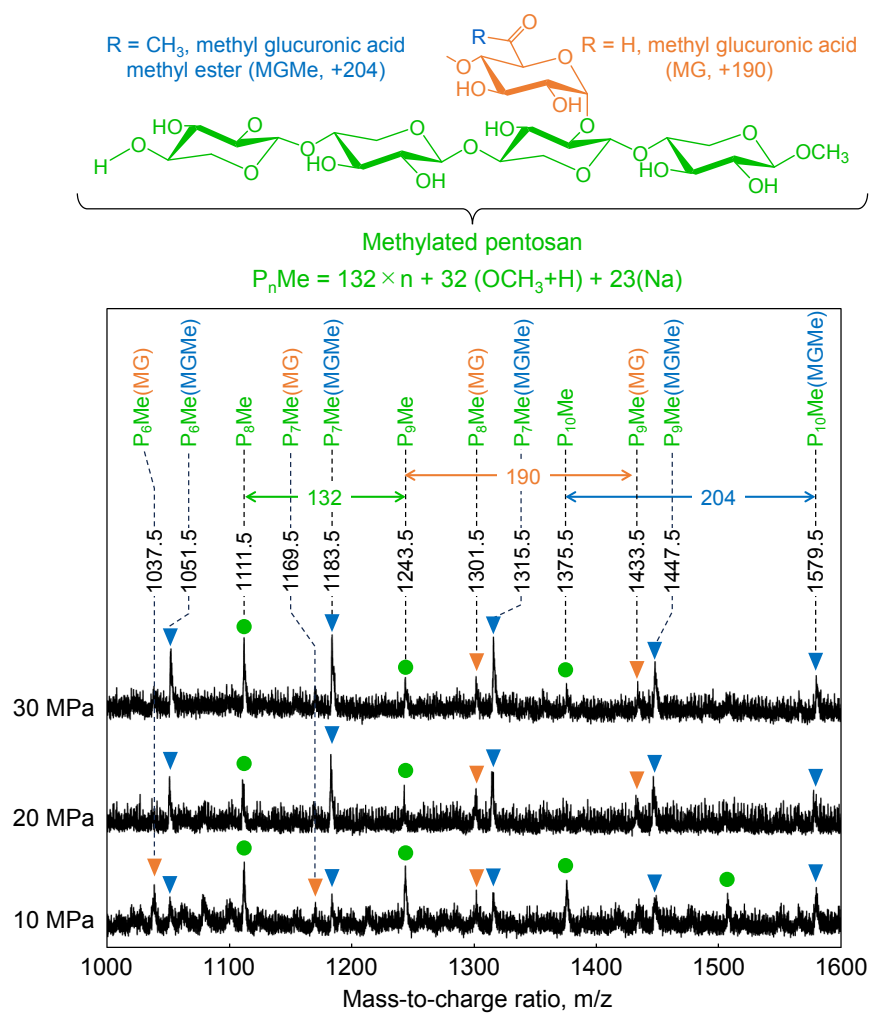


Figure 8

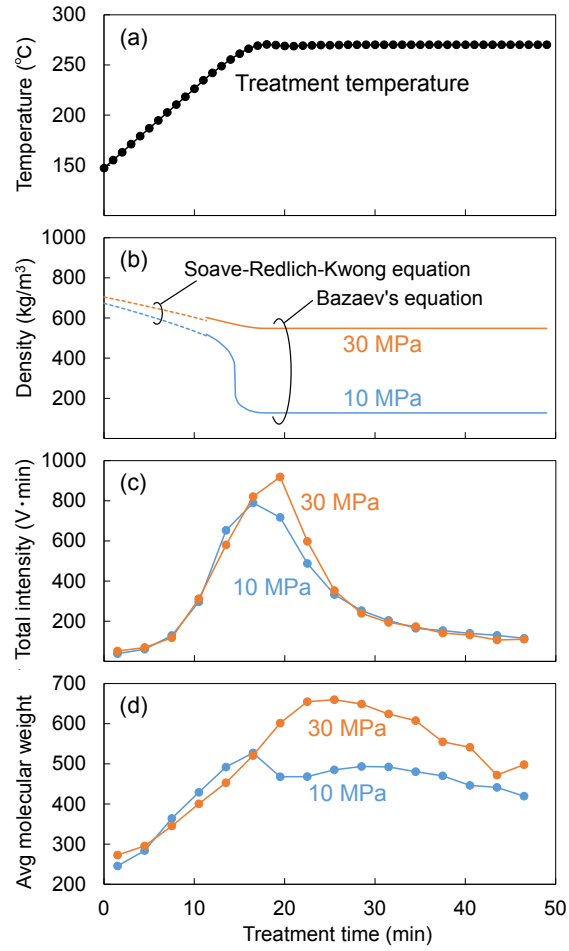


Figure 9



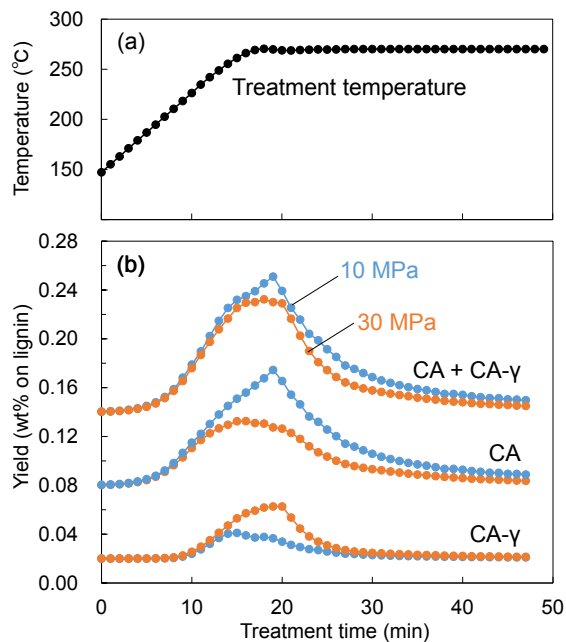


Figure 10



Open Access Article. Published on 14 augusta 2024. Downloaded on 20.8.2024 23:27:57.  
This article is licensed under a Creative Commons Attribution-NonCommercial 3.0 Unported Licence.



Energy Advances Accepted Manuscript

Table 1. Yields of lignin-derived monomers from Japanese cedar wood treated under various conditions.

| Solvent                              | Pressure (MPa) | Flow rate (mL/min) | Yield (wt% on original lignin) |              |          |      |     |      |       |
|--------------------------------------|----------------|--------------------|--------------------------------|--------------|----------|------|-----|------|-------|
|                                      |                |                    | CA                             | CA- $\gamma$ | Vanillin | CAld | IE  | DHCA | Total |
| Methanol/water<br>= 90/10<br>(270°C) | 10             | 5                  | 12.6                           | 2.4          | 1.8      | 1.7  | 0.5 | 0.1  | 19.1  |
|                                      |                | 10                 | 11.4                           | 1.7          | 2.0      | 1.7  | 0.2 | 0.1  | 17.1  |
|                                      |                | 20                 | 11.4                           | 1.2          | 2.1      | 1.9  | nd  | 0.2  | 16.7  |
|                                      | 20             | 5                  | 9.5                            | 2.8          | 1.2      | 1.5  | 0.4 | 0.1  | 15.5  |
|                                      |                | 10                 | 8.3                            | 1.1          | 1.8      | 1.5  | 0.1 | 0.1  | 12.9  |
|                                      |                | 20                 | 6.5                            | 1.6          | 2.3      | 1.8  | nd  | 0.1  | 12.3  |
|                                      | 30             | 5                  | 7.9                            | 3.4          | 1.2      | 1.4  | 0.2 | 0.1  | 14.2  |
|                                      |                | 10                 | 7.2                            | 1.4          | 1.6      | 1.4  | 0.2 | 0.1  | 11.8  |
|                                      |                | 20                 | 5.8                            | 1.4          | 2.3      | 1.8  | nd  | 0.1  | 11.4  |
| Methanol<br>(270°C)                  | 10             | 5                  | 4.1                            | 4.9          | 0.7      | 0.5  | 1.7 | 0.7  | 12.6  |
|                                      | 20             | 5                  | 6.8                            | 3.6          | 0.8      | 0.5  | 0.8 | 0.4  | 12.9  |
|                                      | 30             | 5                  | 6.2                            | 3.8          | 0.6      | 0.4  | 0.9 | 0.3  | 12.2  |
| Water<br>(230°C)                     | 10             | 5                  | 8.2                            | nd           | 1.7      | 1.8  | nd  | 0.6  | 12.3  |
|                                      | 20             | 5                  | 7.9                            | nd           | 1.6      | 1.9  | nd  | 0.6  | 11.9  |
|                                      | 30             | 5                  | 8.3                            | nd           | 1.6      | 1.8  | nd  | 0.6  | 12.2  |

nd, not detected; CA, coniferyl alcohol; CA- $\gamma$ , coniferyl alcohol  $\gamma$ -methyl ether; CAld, coniferyl aldehyde; IE, isoeugenol; DHCA, dihydroconiferyl alcohol





Table 2. Yields of monosaccharides in the hydrolysates of the soluble fractions from Japanese cedar wood treated under various conditions at a flow rate of 5 mL/min.

| Solvent                              | Pressure (MPa) | Yield (wt% on original polysaccharides [cellulose + hemicelluloses]) |                                   |     |     |      |     |     |       |
|--------------------------------------|----------------|--|-----------------------------------|-----|-----|------|-----|-----|-------|
|                                      |                | Solub-<br>ilized   | Recovered neutral monosaccharides |     |     |      |     |     |       |
|                                      |                |  | Glu                               | Man | Xyl | Gala | Ara | Rha | Total |
| Methanol/water<br>= 90/10<br>(270°C) | 10             | 33.4   | 1.2                               | 2.7 | 3.0 | 1.3  | 1.3 | 0.2 | 9.7   |
|                                      | 20             | 24.8   | 1.1                               | 2.4 | 3.2 | 1.3  | 1.2 | 0.2 | 9.4   |
|                                      | 30             | 26.6   | 1.5                               | 2.7 | 3.8 | 1.5  | 1.4 | 0.2 | 11.1  |
| Methanol<br>(270°C)                  | 10             | 24.1   | 0.2                               | 0.4 | 0.4 | 0.4  | 0.7 | 0.1 | 2.2   |
|                                      | 20             | 27.2   | 0.7                               | 0.7 | 0.9 | 0.7  | 0.9 | 0.1 | 4.0   |
|                                      | 30             | 15.4   | 1.0                               | 1.0 | 1.6 | 1.0  | 1.3 | 0.2 | 6.1   |
| Water (230°C)                        | 10             | 44.8   | 3.8                               | 7.5 | 4.4 | 1.1  | 0.8 | 0.2 | 17.8  |

Glu, glucose; Man, mannose; Xyl, xylose; Gala, galactose; Ara, arabinose; Rha, rhamnose; Solubilized, percentage of polysaccharide components in Japanese cedar that were degraded and solubilized in the soluble fraction, evaluated from the results in Figure 2.

